International Journal of Nanomedicine

Dovepress
open access to scientific and medical research

Open Access Full Text Article

ORIGINAL RESEARCH

Synergistic effects of A-B-C-type amphiphilic copolymer on reversal of drug resistance in MCF-7/ADR breast carcinoma

This article was published in the following Dove Press journal:
International Journal of Nanomedicine
11 October 2016
Number of times this article has been viewed

Lu Zhang[1–3]
Jiafei Lu[3]
Liyan Qiu[1]

[1]Ministry of Education (MOE) Key Laboratory of Macromolecular Synthesis and Functionalization, Department of Polymer Science and Engineering, Zhejiang University, Hangzhou, [2]Drug Clinical Trial Office, The First Affiliated Hospital of Wenzhou Medical University, Wenzhou, [3]College of Pharmaceutical Sciences, Zhejiang University, Hangzhou, People's Republic of China

Abstract: P-glycoprotein (P-gp) overexpression has become the most common cause of occurrence of multidrug resistance in clinical settings. We aimed to construct a micellar polymer carrier to sensitize drug-resistant tumors to doxorubicin (DOX). This A-B-C-type amphiphilic copolymer was prepared by the sequential linkage of β-cyclodextrin, hydrophobic poly(D,L-lactide), and hydrophilic poly(ethylene glycol). Upon incubation of the DOX-loaded micelles with DOX-resistant human breast carcinoma MCF-7/ADR cells, significantly enhanced cytotoxicity and apoptosis were achieved. A series of studies on the action mechanism showed that the polymer components such as β-cyclodextrin, hydrophobic poly(D,L-lactide) segment, and poly(ethylene glycol) coordinatively contributed to the improved intracellular ATP depletion and ATPase activity, increased intracellular uptake of P-gp substrates via competitive binding to P-gp, and decreased P-gp expression in MCF-7/ADR cells. More interestingly, a similar phenomenon was observed in the zebrafish xenograft model, resulting in ~64% inhibition of MCF-7/ADR tumor growth. These results implied that the polymeric micelles displayed great potentials as P-gp modulators to reverse DOX resistance in MCF-7/ADR breast carcinoma.

Keywords: multidrug resistance, P-glycoprotein, micelle, doxorubicin, zebrafish

Introduction

Although chemotherapy plays an important role in the clinical treatment of cancer, occurrence of multidrug resistance (MDR) is a crucial factor limiting the effectiveness of chemotherapeutic drugs.[1] According to statistics, MDR has accounted for up to 50% of all cancer-related deaths.[2,3] Currently, varieties of mechanisms of MDR have been posed including enhancement of detoxification systems, activation of DNA repair mechanisms, alteration of drug target structure, and changes in the cellular microenvironment.[4] Among them, the most common cause of MDR in clinics refers to overexpression of P-glycoprotein (P-gp).[5,6] As reported, nearly 40%–50% of patients have P-gp overexpression in the malignant tissues.[7] P-gp functions as an ATP-dependent drug efflux pump and actively transports substrates out of cancer cells,[8,9] which results in decreased intracellular drug concentrations and attenuated sensitivity of tumor cells to drugs.

On the other hand, we have witnessed the explosive development of micelles self-assembled by amphiphilic copolymers as carriers to achieve solubility improvement and selective biodistribution of hydrophobic drugs for cancer treatment. And by means of increasing intracellular uptake, micelles can be helpful to improve the cytotoxicity of drugs to MDR cancers.[10] More notably, Batrakova et al discovered

Correspondence: Liyan Qiu
Ministry of Education (MOE) Key Laboratory of Macromolecular Synthesis and Functionalization, Department of Polymer Science and Engineering, Zhejiang University, 38 Zheda Road, Hangzhou 310027, People's Republic of China
Tel/fax +86 571 8795 2306
Email lyqiu@zju.edu.cn

submit your manuscript | www.dovepress.com
Dovepress
http://dx.doi.org/10.2147/IJN.S115956

that some amphiphilic poly(ethylene oxide)-poly(propylene oxide)-poly(ethylene oxide) block copolymers (Pluronic®) are potent sensitizers of MDR cancer cells as they result in ATP depletion, inhibited P-gp ATPase activity, and decreased microviscosity of the cell membranes.[11] Accordingly, SP1049C containing Pluronic L61 and F127 at a weight ratio of 1:8 became the first P-gp-targeting micellar formulation of doxorubicin (DOX), which has been tested through Phase II clinical evaluation.[12,13] These studies have evoked the deeper exploration on novel functions of amphiphilic copolymers and expanded their application as P-gp modulators in the field of cancer therapy. In addition, they pointed out there exists a close relationship between the polymers' chemical structure and their functions. Namely, some Pluronic products with low hydrophilic–lipophilic balance value display P-gp-modulating activity, such as Pluronic P85 and L61, while others do not, such as Pluronic F127 and F108.[14,15] Afterward, methoxy poly(ethylene glycol)-block-polycaprolactone and d-α-tocopherol poly(ethylene glycol) 1000 succinate were also validated to possess P-gp-inhibitory activity.[16]

Recently, our group has provided some suggestion that micelles integrated with PEGylated polyester and β-cyclodextrin (β-CD) display considerable reversal effects on MRP1-mediated MDR through ATP depletion, mitochondrial membrane potential drop, and GSH content reduction.[17] MRP1 is another important member of ATP-binding cassette transporter family, which can efflux a number of xenobiotics. So far, however, only Pluronic has been reported to have the ability to inhibit both P-gp and MRP1,[11,14,15] indicating that inhibition of the functions of these two efflux pump proteins might be based on different mechanisms. This assumption has been confirmed by Gao et al's study.[18] They designed a novel composite liposomal system co-encapsulating paclitaxel (PTX) and chloroquine phosphate to sensitize PTX-resistant A549/T and A2780/T cancer cells to PTX, and found that this system predominantly inhibited P-gp-mediated efflux but hardly took any effect on MRP1. Therefore, this study aimed to profoundly explore the action mechanism of amphiphilic β-CD-based copolymers to reverse DOX resistance in DOX-resistant human breast carcinoma (MCF-7/ADR) cells with typical P-gp overexpression[19,20] but rare MRP1 expression[21,22] and clarify the intrinsic structure–activity relationships (SARs). First, a linear A-B-C-type amphiphilic copolymer was synthesized by sequentially linking monomethoxy poly(ethylene glycol) (mPEG5000), poly(D,L-lactide), and β-CD. Then, its predominant capability to inhibit P-gp function was investigated through a series of assays including intracellular Rhodamine 123 (Rh123) accumulation, endocytosis pathway, ATP depletion, ATPase activity, P-gp expression, and MDR1 gene expression. Furthermore, the P-gp-overexpressing zebrafish model was initially established to provide more in vivo insights into P-gp inhibition effect of these polymers and resultant enhanced antitumor efficacy.

Materials and methods

Materials

mPEG5000 (number-average molecular weight [MW] 5,000 Da) and D,L-lactide (LA) were obtained from Fluka (Buchs, Switzerland) and Glaco Ltd. (Beijing, People's Republic of China), respectively, and were both dehydrated by azeotropic distillation with toluene for later use. β-CD was purchased from Shanghai Chemical Reagents Co. Ltd. (Shanghai, People's Republic of China) and was recrystallized for later use. Doxorubicin hydrochloride (DOX·HCl; high performance liquid chromatography purity: 98.5%) was obtained from HaiKou Manfangyuan Chemical Company (Hai Kou, People's Republic of China). Rh123 and 3-(4,5-dimethylthiazol-2-yl)-2,5-diphenyl tetrazolium bromide (MTT) were purchased from Sigma-Aldrich Co. (St Louis, MO, USA). R-phycoerythrin-conjugated mouse anti-human monoclonal antibody against P-gp (UIC2) was purchased from Santa Cruz Biotechnology, Inc. (Dallas, TX, USA). P-gp-Glo™ Assay System with P-gp was purchased from Promega Corporation (Fitchburg, WI, USA). Annexin V/propidium iodide (PI) apoptosis kit was purchased from MultiSciences Biotech Co. Ltd (Nanjing, People's Republic of China). Primer pairs and probe were purchased from Sangon Co. Ltd (Shanghai, People's Republic of China). PrimeScript RT Master Mix was purchased from Takara (Otsu, Japan). Fetal bovine serum and Rosewell Park Memorial Institute-1640 medium were purchased from Ji Nuo Biotechnology Company (Hangzhou, People's Republic of China). All other compounds and reagents used were of analytical or high-performance liquid chromatography grade commercially available.

Cell line and culture condition

The Dox-resistant human breast carcinoma (MCF-7/ADR) cell line was obtained from The Cell Bank of Type Culture Collection of Chinese Academy of Sciences and was used as a drug-resistant tumor cell model. Cells were grown in 5% CO_2 at 37°C in the Rosewell Park Memorial Institute-1640 medium containing 10% fetal bovine serum and 1% penicillin/streptomycin. MCF-7/ADR cells were maintained with 1 μg/mL DOX·HCl for 2 weeks to become resistant to DOX before use in the experiments.

Synthesis and characterization of β-CD-modified copolymers

Polymer PELA54-CD containing β-CD was synthesized by polymerization of LA with mPEG5000 and subsequent modification of β-CD.[23,24] First, PELA54 was polymerized by ring opening.[25,26] In brief, a predetermined amount of mPEG5000 and LA at 5:4 weight ratio was added to a dried tube with $Sn(Oct)_2$/toluene (0.5 wt%) as a catalyst, and then toluene was vacuum evacuated and the tube was sealed. The tube was kept at 130°C overnight. When the block copolymer PELA54 cooled and solidified, it was redissolved in anhydrous dichloromethane and precipitated in cold diethyl ether twice to obtain a yield >85%. Then, PELA54 (1 mmol), succinic anhydride (0.12 g, 1.2 mmol), dimethylaminopyridine (0.122 g, 1 mmol), and triethylamine (0.14 mL, 1 mmol) were dissolved in anhydrous 1,4-dioxane and stirred overnight at room temperature. The product was purified twice by ethyl ether, and vacuum-dried overnight to get the white PELA54-COOH powder. The carboxylation of mPEG5000 was done via the same method, and the product was named as mPEG5000-COOH.[21] Next, carbonyldiimidazole-activated[27,28] β-CD (CI-CD) was linked at the end of hydrophobic block of PELA54-COOH or mPEG5000-COOH at a molar ratio of 1:1 at room temperature. β-CD (11.35 mg, 0.01 mmol) and carbonyldiimidazole (6.81 mg, 0.042 mmol) were dissolved in 5 mL dimethyl sulfoxide with 0.01 mol triethylamine, and the reaction was carried out for 3 hours in a dark place under the protection of nitrogen. PELA54-COOH (0.012 mmol) or mPEG5000-COOH dissolved in dimethyl sulfoxide was slowly instilled to CI-CD/DMSO solution with stirring for 24 hours, and then the solution was precipitated in cold ethyl ether, redissolved in dimethylformamide, dialyzed in water for 48 hours, and lyophilized to get the white PELA54-CD or PEG5000-CD powder.

The chemical structure was confirmed by ^{1}H nuclear magnetic resonance (^{1}H NMR) using a Varian 500-MHz NMR spectrometer (Varian Inc., Palo Alto, CA, USA). The proton signals of PELA54-CD, PEG5000-CD, and β-CD were acquired in DMSO-d6 solution, while PELA54 was measured in $CDCl_3$ solution. MW was measured by gel permeation chromatography (GPC) using a Waters GPC system equipped with a Waters Styragel™ HT3 GPC column (Waters, Milford, MA, USA). Tetrahydrofuran acted as both solvent and eluent, and the flow rate was set at 1.5 mL/min. The critical micelle concentration (CMC) which stands for the potential of forming into micelles was studied by pyrene fluorescence measurements.[22] The particle size distribution was studied by Malvern dynamic light scattering (DLS; Nano-S90; Malvern Instruments, Malvern, UK). The shape and morphology of micelles were observed by transmission electron microscopy (JEM-1230; JEOL, Tokyo, Japan).

Preparation and characterization of DOX-loaded polymeric micelles

DOX-loaded polymeric micelles were prepared as previously reported through the method of oil-in-water emulsion.[22] The drug-loaded micelle was lyophilized for future use. DOX in micelles was extracted with dimethylformamide and analyzed with a UV–vis spectrophotometer (TU-1800PC; Purkinje General, Beijing, People's Republic of China) at 482 nm according to the previous studies.[24,29] The particle size of drug-loaded micelles was also studied by DLS. The drug-loaded micelles were subjected to X-ray diffraction (XRD; Bruker D8; Bruker AXS, Billerica, MA, USA) and differential scanning calorimetry (DSC; EXSTAR DSC 7020; SII NanoTechnology Inc., Chiba, Japan) analysis, taking DOX, the blank PELA54-CD micelles, and their physical mixture as controls. The scattering angle of XRD was recorded from 3° to 50°. For DSC, accurately weighed samples were sealed in pan with the heating temperature ranging from 0°C to 260°C at a rate of 5°C/min.

Cell cytotoxicity assay

The in vitro cytotoxicity of various formulations was studied by MTT assay.[30] Following attachment, cells were exposed to blank or DOX-loaded compounds (β-CD, mPEG5000-CD, PELA54, PELA54-CD) at a previously determined set concentration and incubated in thermostatic incubator for 48 hours. Then, 5 mg/mL MTT reagents were added into each well. After incubating for additional 4 hours in thermostatic incubator, the medium was discarded. Thereafter, 200 μL of DMSO was added to dissolve formazan. The plate was measured at 570 nm on a microplate reader (Thermo MK3; Thermo Fisher Scientific, Waltham, MA, USA). The inhibition rate of cell growth was calculated using the formula: Inhibitory rate (%) = $(A_{control} - A_{sample})/A_{control} \times 100$. The cytotoxicity of various compounds was expressed as half maximal inhibitory concentration (IC_{50}) values, which referred to the concentration that caused 50% inhibition of cell growth compared with untreated cells. The resistance reversion index (RRI) was defined as the ratio of IC_{50} of free DOX vs that of DOX-loaded micelles ($RRI = IC_{50,free\ DOX}/IC_{50,micelles}$).[31]

Annexin V-FITC/PI apoptosis assay

The apoptosis induced by DOX-loaded micelles was detected and quantified by the Annexin V-PI apoptosis kit

(MultiSciences Biotech Co. Ltd). Briefly, MCF-7/ADR cells were treated with free DOX·HCl, β-CD/DOX, PEG5000-CD/DOX, PELA54/DOX, and PELA54-CD/DOX (with the DOX concentration of 2 μg/mL). After 48 hours, the control (untreated) and treated cells were harvested, washed, and resuspended in 500 μL ice-cold binding buffer, and then 5 μL Annexin V/FITC solution and 1 μL PI solution were added and incubated at room temperature in the dark for 15 minutes. Then, the cell apoptosis was detected and quantified by flow cytometer (Cytomics FC 500 MCL; Beckman Coulter, Brea, CA, USA).[32]

Intracellular Rh123 accumulation assay

MCF-7/ADR cells were pretreated with a series of concentrations of compounds at 37°C for 1 hour. After that, 2.5 μg of Rh123 was added to each well, and the plates were incubated in the dark for another 1 hour in thermostatic incubator. Then, the plate was taken out, and the cells were washed twice by ice-cold phoshphate-buffered saline (PBS) and lysed with PBS containing 1% Triton X-100 at room temperature. The cell lysate was centrifuged, and Rh123 concentrations in supernatants were measured using a fluorescence microplate reader (SpectraMax M2; Molecular Devices LLC, Sunnyvale, CA, USA) with excitation and emission wavelength of 485 and 530 nm, respectively. Total protein content, determined by bicinchoninic acid protein assay kit (Beyotime Institute of Biotechnology, Shanghai, People's Republic of China), was used to normalize the cellular accumulation of Rh123.[5,14]

Endocytosis pathway studies

To identify the endocytosis pathways of PELA54-CD micelles in MCF-7/ADR cells, the cells were first treated with three specific endocytic inhibitors including chlorpromazine (20 μg/mL),[33] nystatin (15 μg/mL),[34] and amiloride (550 μM)[35] for 1 hour in thermostatic incubator. After that, PELA54-CD/DOX with 10 μg/mL DOX was added and incubated together with inhibitor agents for 2 hours at 37°C. Thereafter, the test solutions were discarded, and the cells were washed by ice-cold PBS thrice. Then, the cells were trypsinized, and the suspension was detected by the flow cytometer with argon ion laser excitation at 488 nm. The report was obtained after analyzing the fluorescent signals of 10,000 cells. The experiment was run in triplicate.

Determination of intracellular ATP

MCF-7/ADR cells were seeded in 24-well plates; after adherance, cells were pretreated with ATP assay buffer for 30 minutes. Then, the assay buffer was replaced with PELA54-CD, PELA54, PEG5000-CD, and β-CD treatment solutions (0.1 or 0.5 mg/mL) in assay buffer for 2 hours. After treatment, cells were washed twice with ice-cold PBS and lysed with ATP lysis buffer on ice. Cell lysate (100 μL) was collected and mixed with ATP assay mix (50 μL) (ATP Assay Kit; Beyotime Institute of Biotechnology). Light emission was studied with a Turner Designs luminometer (Model TD-20/20; Promega Corporation). Data were collected and converted to ATP concentrations according to the guideline. Total protein content was used to normalize ATP levels, and experiments were performed in triplicate.

Measurement of ATPase activity of P-gp

The ATPase activity of P-gp induced by blank micelles was measured via P-gp-Glo™ Assay System kit (Promega Corporation).[36] The assay relied on the ATP-related light-generating reaction of firefly luciferase, which could be detected by luminometer (spectra Max M5; Molecular Devices LLC). ATP consumption of sample was calculated from a standard curve. Specifically, various concentrations of verapamil (control), sodium orthovanadate (Na_3VO_4, acted as a selective inhibitor of P-gp), or different compounds were mixed with recombinant human P-gp membranes in the white opaque 96-well plate (Corning Incorporated, Corning, NY, USA). After preincubation at 37°C for 5 minutes, MgATP was added, and the light-generating reaction started. After sustained reaction at 37°C for 40 minutes, the samples were moved to room temperature, and then ATP detection reagent was added to each hole. The plate was maintained at room temperature for another 20 minutes to develop luminescent signal, and then detected by luminometer. The experiments were performed in triplicate.

Determination of P-gp expression

To measure P-gp levels on the surface of cell, MCF-7/ADR cells were exposed to PELA54-CD, PELA54, PEG5000-CD, and β-CD at 50 μg/mL for 24 hours. R-phycoerythrin-conjugated mouse anti-human monoclonal antibody against P-gp (UIC2) was used to label cells. The fluorescence intensity was analyzed using flow cytometer. The experiments were performed in triplicate.

RT-PCR analysis

MCF-7/ADR cells were treated with PELA54-CD, PELA54, PEG5000-CD, and β-CD at 50 μg/mL for 24 hours and washed twice with ice-cold PBS. Total RNA was extracted by Trizol reagent (Thermo Fisher Scientific, Waltham, MA, USA). The mRNA levels of MDR1 and GAPDH (internal control)

were assessed using real-time reverse-transcription polymerase chain reaction (RT-PCR; Mastercycler®; Eppendorf, Hamburg, Germany). The first strand of cDNA was obtained by reverse transcription with the PrimeScript RT Master Mix (Takara). The primers were designed with software Premier 5.0 and synthesized by Sangon Co. Ltd. The sequences of the primers were as follows: MDR1: forward primer 5′-AAA CAC CAC TGG AGC ATT GAC TAC-3′ and reverse primer 5′-CTG GAA CCT ATA GCC CCT TTAA-3′; GAPDH: forward primer 5′-AGA AGG CTG GGG CTC ATT TG-3′ and reverse primer 5′-AGG GGC CAT CCA CAG TCT TC-3′. The product size was 529 bp. The fluorescent signal was studied using Mastercycler® ep realplex software (Eppendorf). The threshold cycle (CT) number was obtained when PCR amplification reached a significant threshold. The difference in CT value between mdr1 and GAPDH mRNA was defined as ΔCT value. Therefore, ΔCT = (mdr1 mRNA CT) – (GAPDH mRNA CT), and the relative mdr1 mRNA expression level was presented as $2^{-\Delta CT}$. The reaction conditions were set as follows: 95°C for 30 seconds, 30 cycles at 95°C for 5 seconds, and 60°C for 30 seconds, followed by melting curve.[37] Triplicate experiments with triplicate samples were performed.

Rhodamine B-based P-gp activity assay in zebrafish

Zebrafish (AB strain) were maintained in light- and temperature-controlled aquarium with a system on a 14-hour/10-hour light/dark cycle and fed according to standard protocols.[38] In general, 200–300 embryos were collected from nature mating of four to five pairs of zebrafish each time, and were incubated at 28°C in specific fish water, washed, and staged at 6 or 24 hours postfertilization (hpf). The experiments involving zebrafish were conducted in line with animal care guidelines authorized by the Association for Assessment and Accreditation of Laboratory Animal Care International.

To evaluate the effect of PELA54-CD on P-gp, 4 hpf zebrafish were co-treated with seven different concentrations (0.1, 1, 10, 100, 250, 500, and 1,000 mg/L) of PELA54-CD and Rhodamine B for 20 hours. Cyclosporine A served as a positive control drug. Zebrafish treated with Rhodamine B were used as control. After treatment, ten randomly selected zebrafish from each group were imaged under a stereo fluorescent microscope (AZ100; Nikon Corporation, Tokyo, Japan). Through image-based morphometric analysis, the quantitative fluorescent signal data (S) were obtained and expressed as mean ± standard error (SE) (n=10). Inhibitory efficiency of PELA54-CD on P-gp was calculated using the following formula: P-gp inhibition (%) = $(S_{\text{PELA54-CD}}/S_{\text{control}} - 1) \times 100$.

P-gp protein expression assay in zebrafish

After PELA54-CD treatment, zebrafish embryo total protein was extracted, and the protein concentration of lysates was meatured by Protein Assay Dye Reagent Concentrate (Bio-Rad Laboratories Inc., Hercules, CA, USA). Fifty micrograms of each lysate sample was separated by 4% sodium dodecyl sulfate-polyacrylamide gel electrophresis and transferred onto a nitrocellulose membrane (Pall Corporation, Port Washington, NY, USA). After blocking with 5% fat-free milk for 24 hours at 4°C, primary mouse anti-human monoclonal antibody (1:200; GeneTex, Inc., Irvine, CA, USA) was added followed by the secondary antibody (1:10,000, anti-mouse IgG-HRP, incubated at room temperature for 1 hour). At last, reactive P-gp was visualized by electrochemiluminescence system (Thermo Fisher Scientific).

P-gp gene expression assay in zebrafish

After PELA54-CD treatment, zebrafish embryo total RNA and total protein were extracted. Total RNA was reverse-transcribed using ReverTra Ace-α-RT Kit (Toyobo, Osaka, Japan) to perform RT-PCR, and β-actin was used as the reference gene. 2X Taq Master Mix (Bio Life Inc., Shanghai, People's Republic of China) kit was used for the PCR using a thermal cycler (Bioer, Hangzhou, People's Republic of China) as follows: 94°C for 2 minutes; 26 and 34 cycles (MDR1 and β-actin, respectively) of 94°C for 30 seconds, 56°C for 30 seconds, and 72°C for 30 seconds; and 72°C for 10 minutes. The expected size of the MDR1 and β-actin fragments was 243 and 389 bp, respectively. After agarose electrophoresis, Launch SensiAnsys (Peiqing Inc., Shanghai, People's Republic of China) was used to quantify the intensity of DNA bands (S). Inhibitory efficiency of PELA54-CD on MDR1 gene expression was analyzed using the equation: MDR1 gene expression Inhibition (%) = $(1 - S_{\text{compound}}/S_{\text{control}}) \times 100$.

Xenografts in zebrafish

AB strain zebrafish was used to study the inhibition of PELA54-CD/DOX on the growth of xenografts of MCF-7/ADR cells. Approximately 400–500 MCF-7/ADR cells labeled with CM-Dil (V-22885; Thermo Fisher Scientific) were microinjected into the yolk sac of 48 hpf embryos. PELA54-CD/DOX, DOX·HCl, or PBS as blank was microinjected into the pericardium 24 hours later. Anesthetized zebrafish were imaged both before and 48 hours

after injection of different drugs. The fluorescent signal (S) obtained from images represented the growth of MCF-7/ADR cells, and the inhibition rate was calculated using the equation: Inhibition rate of growth (%) = $(1 - S_{PELA54\text{-}CD/DOX}/S_{control}) \times 100$. Results are presented as mean ± SE from ten independently performed experiments.

Statistical analysis

Statistical analysis was performed using SPSS 11.5 software. Statistical significance was considered at $P<0.05$.

Results and discussion

Synthesis and characterization of polymeric compounds

A series of amphiphilic copolymers were synthesized including PEG5000-CD, PELA54, and PELA54-CD compounds (Figure S1). The copolymer designated as PELA54-CD contained PELA54 blocks with a 5:4 (w/w) feed ratio of mPEG5000 and LA.

The chemical structures of various polymeric compounds were characterized by ^{1}H NMR. Taking as examples, the ^{1}H NMR spectra shown in Figure 1 integrated those peaks characteristic of PELA54-CD, PELA54, PEG5000-CD, and β-CD. The peaks at δ 1.47 ($-CH_3$) and δ 5.21 (–CH) were attributed to poly(D,L-lactide) (PLA) blocks, while peaks at δ 3.51 ($-CH_2$) and δ 3.24 ($-OCH_3$) were attributed to mPEG5000 blocks. The peak at δ 4.83 was typical of the C1 hydrogen of β-CD. The conjugation ratio of PELA54 to β-CD was found to be ~1.1 by calculating the peak area ratio of $-OCH_3$ (δ 3.24) to C1 hydrogen (δ 4.83).

The MW of PELA54 was calculated as 9,582 according to the integral values of peak area of –CH (δ 5.21) and $-OCH_3$ (δ 3.24) in ^{1}H NMR spectrum. Then, based on the MW of PELA54 and the conjugation ratio, the MW of PELA54-CD was calculated as 11,675, which was consistent with the data measured by GPC (Table 1).

The surfactant concentration at which micelles form is termed as CMC. Therefore, as shown in Table 1, β-CD could not form micelles, while the CMC of PEG5000-CD was calculated to be 0.028 mg/mL, suggesting that PEGylated β-CD could self-assemble into nanoparticles with a size of 165 nm. Notably, once hydrophobic PLA segment was introduced, the CMCs of PELA54-CD aggregates significantly decreased (0.00112 mg/mL) compared with that of PEG5000-CD, which could facilitate the stability of micelles in blood circulation. Therefore, the polymers with a concentration >10 μg/mL used in the following assays were in the state of self-assembled micelles. The transmission electron microscopy images in Figure S2 displayed uniform size distribution of PELA54-CD micelles with a relatively smooth surface.

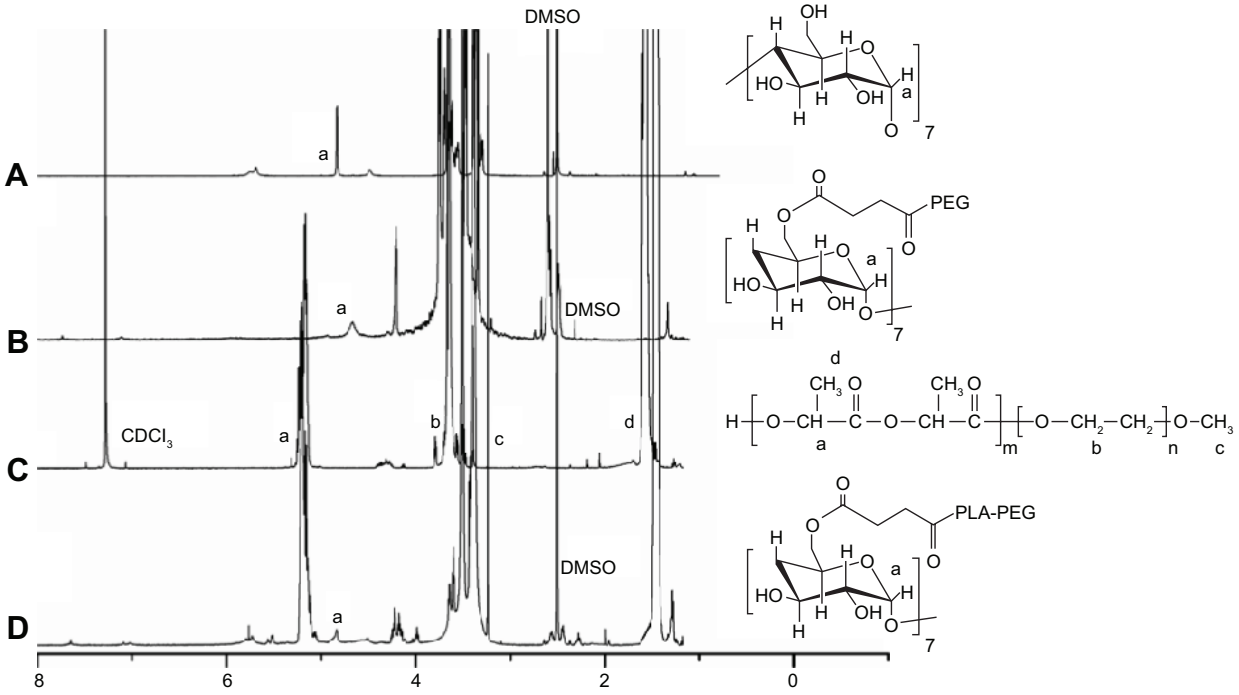

Figure 1 ^{1}H NMR spectra of different compounds.
Notes: (**A**) β-CD in DMSO-d6. (**B**) PEG5000-CD in DMSO-d6. (**C**) PELA54 in $CDCl_3$. (**D**) PELA54-CD in DMSO-d6.
Abbreviations: NMR, nuclear magnetic resonance; CD, cyclodextrin; DMSO, dimethyl sulfoxide; mPEG5000, poly(ethylene glycol); PELA54, 5:4 monomethoxy poly(ethylene glycol):D,L-lactide; PLA, poly(D,L-lactide); β-CD, beta-cyclodextrin.

Table 1 Characterization of various polymeric compounds

Polymers	Feed ratio[a]	Mn[b]	Mn[c]	Mw[c]	PDI[c]	CMC (mg/mL)	Particle size (nm)	
							Blank micelles	DOX-loaded micelles
PELA54-CD	5:4	11,675[b]	12,003	14,044	1.17	0.00112	134±21.3	135.3±23.7
PEG5000-CD	–	6,135	5,809	6,858	1.37	0.028	165±15.3	164.0±25.0
PELA54	5:4	9,582[b]	8,743	9,062	1.04	0.00167	80±13.9	135.0±21.6
β-CD	–	1,135	–	–	–	–[d]	–[d]	300.0±50.6[e]

Notes: [a]Feed ratio of mPEG5000 to LA or CL (g/g). [b]Calculated from the ^{1}H NMR spectra. [c]Measured via gel permeation chromatography. [d]Not detected. [e]Not micelles. Data presented as mean ± standard deviation.

Abbreviations: Mn, number-average molecular weight; Mw, weight-average molecular weight; PDI, polydispersity index; CMC, critical micelle concentration; DOX, doxorubicin; PELA54, 5:4 monomethoxy poly(ethylene glycol):D,L-lactide; CD, cyclodextrin; mPEG5000, poly(ethylene glycol); β-CD, beta-cyclodextrin; LA, D,L-lactide; CL, caprolactone; NMR, nuclear magnetic resonance.

Preparation and characterization of DOX-loaded polymeric micelles

The drug-loading content of PELA54 and PELA54-CD micelles was set at ~12% (encapsulation efficiency >85%) in order to supply similar condition for the subsequent cytotoxicity assay. Due to the limited loading ability, the DOX-loading content of β-CD and PEG5000-CD could only reach 3.4% and 8.9%, respectively. The enhanced drug loading of PELA54-CD was attributed to the cooperation of the β-CD inclusion effect and the hydrophobic interactions of PLA with DOX.[23,24] The particle sizes of the resultant DOX-loaded micelles were distributed between 130 and 170 nm determined by DLS (Table 1) which was small enough to be transported from blood circulation to the tumor site via enhanced permeability and retention effect and further taken up by tumor cells after intravenous injection. Due to the inclusion action between β-CD and DOX, the particle size did not change much for DOX-loaded PELA54-CD or PEG5000-CD micelles in comparison to the corresponding blank micelles.

DSC and XRD analyses on DOX·HCl, PELA54-CD, physical mixtures of DOX·HCl and PELA54-CD, and lyophilized PELA54-CD/DOX were conducted in order to determine the physical existing status of DOX in PELA54-CD micelles. The melting endothermic peak of DOX·HCl appeared at ~225°C in both free DOX·HCl and physical mixtures, but it disappeared in lyophilized PELA54-CD/DOX (Figure S3). As shown in Figure S4, the crystalline peaks of DOX·HCl can be clearly observed in DOX·HCl and the mixture powder; however, these peaks are absent in the spectra of DOX-loaded micelles. These results suggested that DOX was essentially amorphous after encapsulated into the micelles.

Cytotoxicity and apoptosis assay

The influence of various preparations on DOX-induced cytotoxicity was tested by MTT assay against MCF-7 and MCF-7/ADR cells. The IC_{50} values of free DOX at 48 hours were 0.30 and 20.937 μg/mL in MCF-7 and MCF-7/ADR cells, respectively, suggesting that MCF-7/ADR cells possessed considerable resistance to DOX. No polymers in the dose tested range showed any inherent toxicity (<5% cell death) to either cell lines (data not shown), suggesting that they would not interfere with the MTT assay against cells treated with DOX-loaded formulations. As shown in Figure 2A, the cytotoxicity of DOX was improved in the following order: DOX·HCl < PEG5000-CD/DOX ≈ β-CD/DOX < PELA54/DOX < PELA54-CD/DOX. The action of the various formulations on the resistant cells (MCF-7/ADR) was quantitatively expressed in the form of RRI.[39] Consistent with Figure 2A, the RRI of β-CD/DOX was the lowest at 1.89, while that of PELA54-CD/DOX was the highest at 8.82. These data suggested that any part of β-CD, mPEG5000, or PLA could contribute separately to sensitize DOX-resistant cells but that their combination was the best (Table 2).

The DOX-induced apoptosis was also evaluated. Figure S5 shows that, after treatment for 48 hours, the percentage of apoptotic cells in free DOX·HCl (2 μg/mL) was 12.25%. When DOX was included into β-CD, the apoptosis ratio increased to 16.96%. But the apoptosis ratio of DOX-loaded micelles was further improved and markedly higher than that of free DOX·HCl in the order: PELA54-CD/DOX (30.11%) > PELA54/DOX (24.09%) > PEG5000-CD/DOX (20.48%) > β-CD/DOX (16.96%) > DOX·HCl (12.25%) (Figure 2B). These results were in line with the cytotoxicity test. PELA54-CD micelles with the hydrophobic PLA segments produced the most significant cell cytotoxicity.

Intracellular accumulation of Rh123

As metioned above, the DOX-induced cytotoxicity and apoptosis displayed some regular dependence on the chemical structure of amiphilic polymers. This phenomenon reminded us that polymeric carriers themselves probably exerted certain actions to inhibit DOX efflux of P-gp, which was related to DOX resistance reversal of MCF-7/ADR cells.

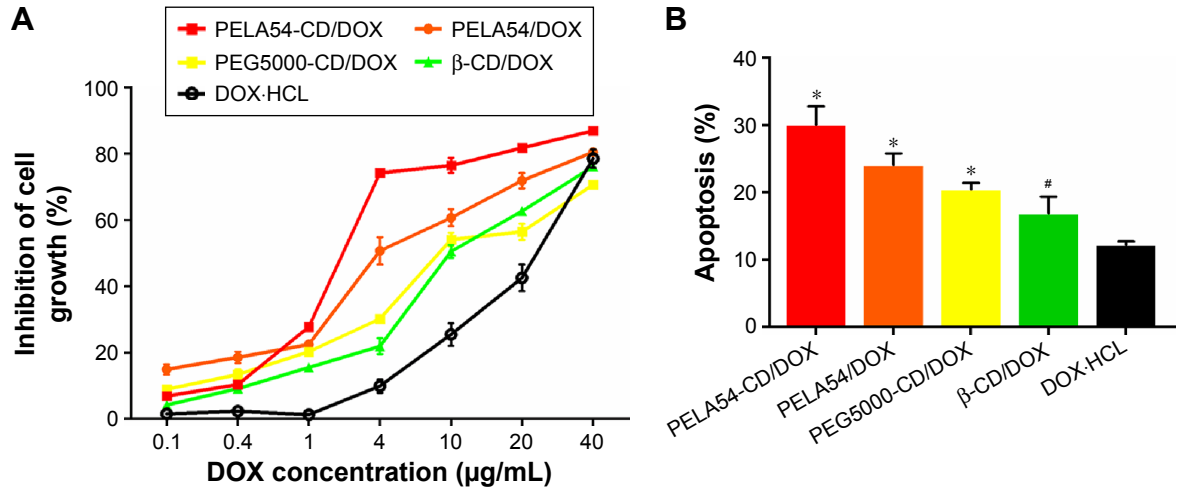

Figure 2 Cytotoxicity and apoptosis studies against MCF-7/ADR cells.
Notes: (**A**) Cytotoxicity of different formulations containing DOX against MCF-7/ADR cells for 48 hours. (**B**) Percentage of DOX-induced apoptosis in MCF-7/ADR cells detected by flow cytometry after 48 hours. *$P<0.01$ and #$P<0.05$, compared with DOX·HCl. The results are represented as mean ± SD (n=3).
Abbreviations: DOX, doxorubicin; SD, standard deviation; PELA54, 5:4 monomethoxy poly(ethylene glycol):D,L-lactide; CD, cyclodextrin; mPEG5000, poly(ethylene glycol); β-CD, beta-cyclodextrin.

To investigate whether polymers could affect P-gp function, the effects of various polymers on the cellular accumulation of Rh123, a classical substrate of P-gp, in MCF-7/ADR cells were determined.[40,41]

Figure S6 shows that all tested polymers enhanced intracellular Rh123 accumulation in MCF-7/ADR cells until the polymer concentrations increased to a certain value, after which Rh123 accumulation began to decrease. This concentration-related pattern was consistent with the report about the influence of Pluronic block copolymers on Rh123 accumulation.[42] It is interesting to notice that these carriers could improve the cellular uptake of Rh123. But compared with β-CD, PEG5000-CD, and PELA54, PELA54-CD micelles achieved the highest cellular uptake of Rh123, which was more than twice as much as that of controlled group (free Rh123) (Figure 3). This phenomenon verified that PELA54-CD polymers could affect P-gp function, resulting in the improved cytotoxicity and apoptosis in P-gp-overexpressed cells.

Table 2 IC_{50} and RRI of various formulations against MCF-7/ADR cells

Formulations	IC_{50} (μg/mL) (mean ± SD, n=3)	RRI
Free DOX·HCl	20.937±1.881	–
β-CD/DOX	11.100±1.040	1.89
PEG5000-CD/DOX	10.657±1.029	1.96
PELA54/DOX	4.573±0.603	4.58
PELA54-CD/DOX	2.376±0.167	8.82

Abbreviations: IC_{50}, half maximal inhibitory concentration; RRI, resistance reversion index; SD, standard deviation; DOX, doxorubicin; CD, cyclodextrin; mPEG5000, poly(ethylene glycol); PELA54, 5:4 monomethoxy poly(ethylene glycol):D,L-lactide; β-CD, beta-cyclodextrin.

Action mechanisms of PELA54-CD copolymers in MDR cells

Enhanced intracellular accumulation of Rh123 confirmed that PELA54-CD micelles themselves could inhibit P-gp-induced substrate efflux. Therefore, the following studies were focused on providing insight into the action mechanisms of these polymers to reverse MDR in MCF-7/ADR cells, which involved the assay of endocytosis pathway, ATP depletion, ATPase activity, P-gp expression, and MDR1 gene expression.[43–45]

Endocytosis pathways of PELA54-CD/DOX

Miller et al[46] suggested that the P-gp-independent absorption process of Pluronic P85 micelle observed in bovine brain

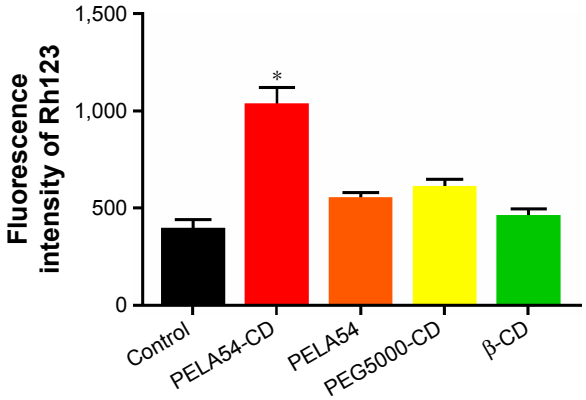

Figure 3 The cellular accumulation of Rh123 in MCF-7/ADR cells in the presence of 0.1 mg/mL PELA54-CD, PELA54, PEG5000-CD, and β-CD.
Notes: The results are represented as mean ± SD (n=3). Statistical significance (*$P<0.01$) was compared with control group.
Abbreviations: Rh123, Rhodamine 123; PELA54, 5:4 monomethoxy poly(ethylene glycol):D,L-lactide; CD, cyclodextrin; mPEG5000, poly(ethylene glycol); SD, standard deviation; β-CD, beta-cyclodextrin.

microvessel endothelial cell monolayers was attributed to endocytosis, and therefore, the endocytosis pathways of PELA54-CD micelles were studied. Nanoparticles can be uptaken by cancer cells via different endocytosis pathways, namely caveolae-mediated endocytosis, clathrin-mediated endocytosis, and macropinocytosis.[47] Caveolae-mediated endocytosis could transport nanoparticles to the nucleus via cavicles and avoid fusion with the degradative lysosome. However, clathrin-mediated endocytosis pathway leads nanoparticles into early endosomes, which ends up with lysosomal fusion. Macropinocytosis is a solute concentration-based endocytosis for fluid-phase matter around the cells.[48] For the purpose of identifying the endocytosis pathway of DOX-loaded PELA54-CD micelles, inhibitors of caveolae-mediated endocytosis (nystatin), clathrin-mediated endocytosis (chlorpromazine), and macropinocytosis (amiloride) were used in the 2-hour uptake studies. The results showed that in comparison with uptake of PELA54-CD/DOX in the absence of endocytosis inhibitors as control, chlorpromazine did not lead to reduction in cellular uptake of DOX,[40,49–51] while nystatin and amiloride decreased the cell endocytosis (Figure S7). Therefore, the study demonstrated the involvement of caveolae- and macropinocytosis-dependent and clathrin-independent endocytosis of the PELA54-CD micelles in MCF-7/ADR cells, which was desirable for achieving endosomal escape into the cytoplasm of the cells.

Effects of micelles on intracellular ATP

Cellular energy consumption could be one reason of the inhibition of P-gp function since drug efflux is energy-dependent. Hence, the intracellular levels of ATP in MCF-7/ADR cells were measured using ATP assay kit after incubation with a series of compounds for 2 hours. Figure 4 shows that the employment of β-CD, PEG5000-CD, and PELA54 hardly decreased cellular ATP levels in MCF-7/ADR cells. However, the exposure to PELA54-CD at 0.1 mg/mL resulted in significant decrease of ATP level to 70%–80%. As more PELA54-CD (0.5 mg/mL) was applied, more ATP depletion (ATP level decreased to 50%–60%) was observed. The typical phenomenon was observed in the case of Pluronic P85. When MCF-7/ADR cells were exposed to Pluronic P85, the ATP level was gradually decreased with the increase of polymer concentration until it dropped to ~3.8% at the Pluronic P85 concentration of 0.05 wt%.[11] It is reported that in many cases, drug transport is very sensitive to ATP depletion and requires an ATP-regenerating system for maximal transport.[52–54] As for MDR cells, drug efflux process is seriously ATP-dependent. Though the ATP-level decrease

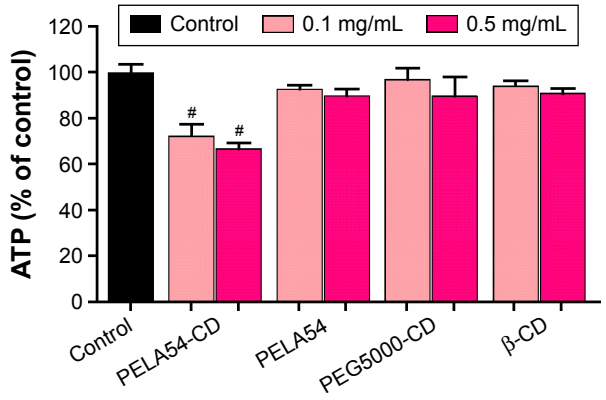

Figure 4 Effects of micelles on the intracellular ATP level.
Notes: Cells were incubated with different polymers at the concentration of 0.1 or 0.5 mg/mL for 2 hours. The data are presented as percent of the untreated control. The results are represented as mean ± SD from three independent experiments (n=3). Statistical significance ($^{\#}P<0.05$) was compared with control group.
Abbreviations: SD, standard deviation; PELA54, 5:4 monomethoxy poly(ethylene glycol):D,L-lactide; CD, cyclodextrin; mPEG5000, poly(ethylene glycol); β-CD, beta-cyclodextrin.

caused by PELA54-CD was much weaker than that caused by Pluronic P85, it is still reasonable to assume that the energy depletion in PELA54-CD micelle-treated group could reduce the energy supply for P-gp efflux, and consequently, improve cytotoxicity of DOX.

Regulation of P-gp ATPase activity

P-gp is considered structurally as a "full transporter". It transports substrate in two ways: one goes through a passage within the inner leaflet of the membrane and one goes through a passage at the cytoplasmic side in which ATP binds. After binding of substrate and ATP, P-gp ATPase hydrolyzes ATP and transfers the substrate out of cell. Several groups[48,55] have investigated carefully about the substrate-binding pattern and the correlation between ATPase hydrolysis and P-gp transport mechanism. Therefore, ATPase activity reflects the relationship between compounds and the P-gp-mediated drug efflux. P-gp substrates usually partition into the membrane, compete for a common pharmacophore present in P-gp,[56] and continuously stimulate P-gp ATPase activity, while P-gp inhibitors such as Pluronic P85[11] inhibit the basal P-gp ATPase activity.[57–60] To confirm that the inhibition of P-gp-induced drug efflux by polymeric PELA54-CD micelle was related to interfere with P-gp ATPase activity, P-gp-Glo™ Assay was performed.

Na_3VO_4 is a selective inhibitor of P-gp.[59] ATP consumption in the presence of Na_3VO_4 is attributed to minor non-P-gp ATPase activities in membrane system supplied by the kit. The known P-gp substrate verapamil served as a positive control. The luminescence of the samples was recorded using SpectraMax M5 microplate reader.

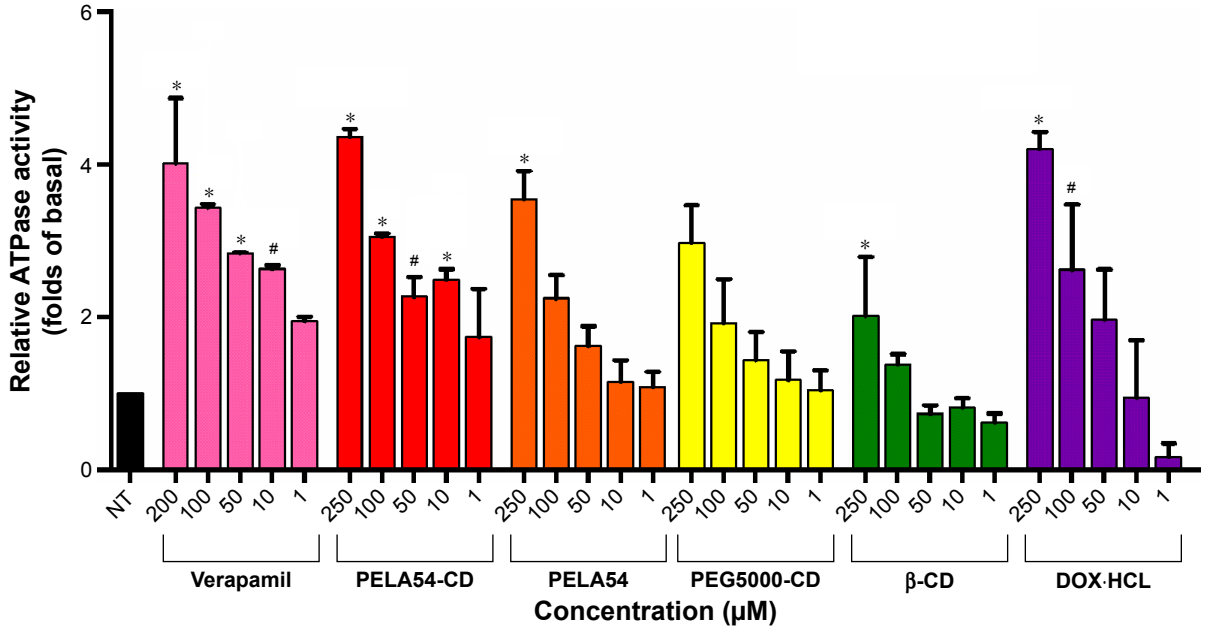

Figure 5 Stimulation of P-gp ATPase activity by polymers as compared with verapamil and DOX·HCl.
Notes: Data were analyzed in terms of ATPase activity by comparison to the ATP standard curve. The results are represented as mean ± SD (n=3). Statistical significance ($^{\#}P<0.05$ and $^{*}P<0.01$) was compared with untreated samples (NT) group.
Abbreviations: P-gp, p-glycoprotein; DOX, doxorubicin; SD, standard deviation; PELA54, 5:4 monomethoxy poly(ethylene glycol):D,L-lactide; CD, cyclodextrin; mPEG5000, poly(ethylene glycol); β-CD, beta-cyclodextrin.

ATPase activities (pmol/min/μg protein) of polymer-treated samples were compared with the ATPase activities of samples treated with both verapamil and DOX·HCl. The decrease in luminescence of untreated samples (NT) compared with Na_3VO_4-treated samples was defined as basal activity. As shown in Figure 5, compared with the NT group, verapamil, DOX·HCl, PELA54-CD, PELA54, and PEG5000-CD all significantly increased the ATPase activity in a concentration-dependent manner.

The various concentrations of compounds in ATPase activity assay displayed optimum curves of stimulation, and their activities conformed to the classical Michaelis–Menten competition equation, suggesting that all of the compounds are substrates for transport by P-gp.[59] In order to quantify the interactions of the compounds with P-gp, all ATPase activity assay data were analyzed through double reciprocal plots according to Lineweaver and Burk[61] to obtain maximal reaction rate (*V*m) and apparent Michaelis constant (*K*m). *K*m is identified to indicate the affinity between an enzyme and its substrate; the lower *K*m represents a higher affinity in enzymology.[62,63] As shown in Table 3, the order of *K*m values was verapamil < PELA54-CD < PELA54 < PEG5000-CD < β-CD < DOX·HCl. Among the compounds, the well-known chemosensitizer verapamil stimulated the ATPase activity by 1.9- to 4-fold above basal (1–250 μM) with a *K*m of 0.676 μM, while the PELA54-CD micelle yielded a 1.7- to 4.4-fold stimulation of ATPase activity with a *K*m of 0.704 μM. DOX·HCl stimulated the ATPase activity by 0.2- to 4.2-fold over basal with a higher *K*m of 3.873 μM. Comparing all the *K*m values, the combination of mPEG5000, PLA, and β-CD in the polymers evidently contributed to the decreased *K*m value, which made PELA54-CD micelle display higher affinity to P-gp than DOX·HCl.

Previous study showed that a number of widely used synthetic polymeric pharmaceutical agents can modulate the function of efflux pumps,[44] especially PEGylated surfactants.

Table 3 Kinetic parameters of P-gp ATPase activity stimulated by verapamil, various polymers, β-CD, and DOX·HCl

Samples	Verapamil	PELA54-CD	PELA54	PEG5000-CD	β-CD	DOX·HCl
*K*m (μM)	0.676	0.704	0.784	0.885	1.1484	3.873
*V*m (pmol/min/μg protein)	54.054	49.261	32.787	30.211	64.516	71.942

Notes: The analysis was done according to the Lineweaver–Burk plot of the corrected result in ATPase activity assay. *K*m and *V*m values were calculated.
Abbreviations: P-gp, P-glycoprotein; CD, cyclodextrin; DOX, doxorubicin; PELA54, 5:4 monomethoxy poly(ethylene glycol):D,L-lactide; mPEG5000, poly(ethylene glycol); *K*m, apparent Michaelis constant; *V*m, maximal reaction rate; β-CD, beta-cyclodextrin.

Furthermore, early SAR studies analyzing P-gp modulators pointed to their features of lipophilicity, long axis of the molecule of minimum 18 carbon atoms, nucleophilicity, and cationic charges.[64,65] Therefore, the hydrophobic self-assembled region formed by polymeric segment PLA, hydrophobic chamber of β-CD, and the long carbon chain in mPEG5000 in polymeric micelles coordinatively conformed to the SAR with P-gp. Usually, not only one substrate molecule can bind to P-gp at the same time, and different substrates can allosterically modulate each other's transport.[66,67] Based on the ATPase activity analysis and *K*m value calculation, PELA54-CD micelle with higher affinity to P-gp can effectively inhibit the efflux of other P-gp substrates like DOX as a competitive substrate.

Regulation of P-gp and MDR1 gene expression

Sachs-Barrable et al[66] reported the decrease of P-gp protein expression in Caco-2 cells and the downregulation of MDR1 after treatment with two lipid excipients Peceol™ and Gelucire® 44/14 which had the ability to reduce P-gp-mediated efflux, suggesting that more than just depletion of ATP or alteration of ATPase activity, decrease of protein or gene expression is responsible for P-gp efflux function inhibition. Therefore, in order to confirm whether polymers based on β-CD could downregulate P-gp expression on the cellular surface, the protein level in cells was analyzed by flow cytometry. As shown in Figure S8, MCF-7/ADR cells exhibited a strong fluorescent area (35.1%) which represented high level of P-gp expression, while MCF-7 cells showed almost no fluorescent signal (2%). After 24-hour incubation with PELA54, PEG5000-CD, and PELA54-CD micelles at 50 μg/mL, the fluorescent signal was significantly decreased. It is also obvious that PELA54-CD was the most active micelle since it downregulated the expression of P-gp by >50%, compared with that in the control group (Figure 6). However, PELA54, PEG5000-CD, and β-CD only moderately downregulated the expression. These results again illustrated the value of the combination of mPEG5000, PLA, and β-CD in one polymer to decrease the expression of P-gp in drug-resistent MCF-7/ADR cells.

By real-time quantitative RT-PCR, examination was done on whether polymer-induced decrease of P-gp was related to the lessened expression of MDR1 gene, which encodes P-gp drug efflux pump. Treatment with verapamil (50 μg/mL) resulted in ~50% decrease in MDR1 gene expression level compared with the control. However, the incubation of MCF-7/ADR cells with various polymers at 50 μg/mL for 24 hours did not significantly influence the expression level of MDR1 gene (data not shown). Considering the result of decreased P-gp expression and unchanged MDR1 gene, it was presumed that the micelles could affect the translation process of mRNA and/or modification which was a common phenomenon as reported previously.[68]

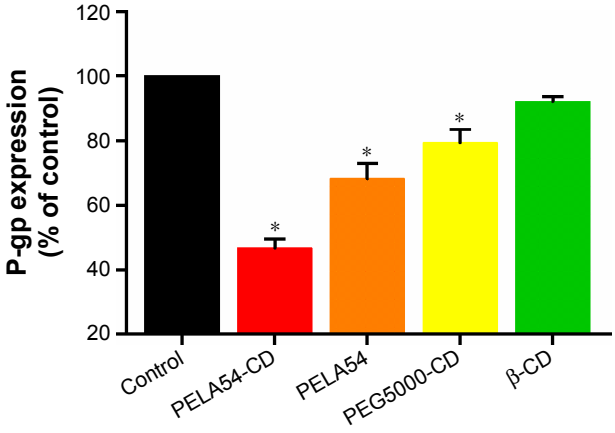

Figure 6 P-gp expression in the surface of MCF-7/ADR cells after exposing to different polymers (PELA54-CD, PELA54, PEG5000-CD, β-CD) at 50 μg/mL for 24 hours.
Notes: The data measured by FCM are presented as percent of the untreated MCF-7/ADR control. The results are represented as mean ± SD (n=3). Statistical significance (*$P<0.01$) was compared with control group.
Abbreviations: P-gp, p-glycoprotein; PELA54, 5:4 monomethoxy poly(ethylene glycol):D,L-lactide; CD, cyclodextrin; mPEG5000, poly(ethylene glycol); FCM, flow cytometry; SD, standard deviation; β-CD, beta-cyclodextrin.

Zebrafish in vivo assessment of PELA54-CD inhibition on P-gp

All the formulations (β-CD, PEG5000-CD, PELA54, PELA54-CD) were studied using in vitro experiments, and the results showed that PELA54-CD displayed the best effect of inhibiting the function of P-gp-mediated drug efflux. On this basis, in vivo studies were performed using PELA54-CD, and focus was on the dose–activity relationship between the polymeric carriers and drug resistance reversal.

The establishment of zebrafish model offered new opportunity to study the molecular mechanisms of various human diseases and helped to verify novel drug targets. Until now, xenograft models of solid tumor such as colon/breast/stomach/prostate/brain/pancreatic cancer, as well as leukemia and melanoma have been built by microinjection of cancer cell lines into pericardium, abdominal perivitelline space, or the yolk sac of 2-day postfertilization zebrafish embryos.[69] These models are relatively economic, simple, and reproducible when launching large-scale animal experiments.[69,70] In addition, the transparent body of zebrafish is quite suitable for in vivo observation of fluorescently tagged drugs or cells. To meet the requirement of this study, stable P-gp-overexpressing AB strain zebrafish were used in the following experiments.[70]

Rhodamine B-based P-gp activity assay in zebrafish

After co-treatment with PELA54-CD at seven concentrations (0.1–1,000 mg/L) and 6 μM Rhodamine B for 20 hours, the red fluorescence of Rhodamine B gradually became stronger (Figure 7A). Particularly, at 1,000 mg/L PELA54-CD, the fluorescence strength exceeded that in positive control (1,000 mg/mL cyclosporine A). These images and data showed that PELA54-CD helped to inhibit Rhodamine B effluxed via P-gp in zebrafish in a concentration-dependent mode (Figure 7B), which was in accordance with the result of intracellular accumulation of R123 in in vitro model of MCF-7/ADR cells.

P-gp protein expression and gene assay in zebrafish

To test whether PELA54-CD had the ability to affect P-gp expression in the zebrafish model, Western blotting and RT-PCR were performed. Interestingly, a downregulation of the protein expression was observed upon treatment with PELA54-CD (Figure 7C and D), but the MDR1 expression level was not altered significantly (data not shown). This result was in line with the in vitro result of protein expression and gene transcription. The micelles could affect the translation process of mRNA and/or modification, which is reported in previous research.[68]

Xenografts in inhibition in zebrafish

CM-Dil-labeled MCF-7/ADR cells were microinjected into the yolk sac of 48 hpf embryos to generate the xenografts model. The fluorescence signal (*S*) of zebrafish xenografts of MCF-7/ADR cells was obtained, without interference from the natural fluorescence of DOX (displayed in Figure S9). The xenografts of MCF-7/ADR cells treated with DOX·HCl

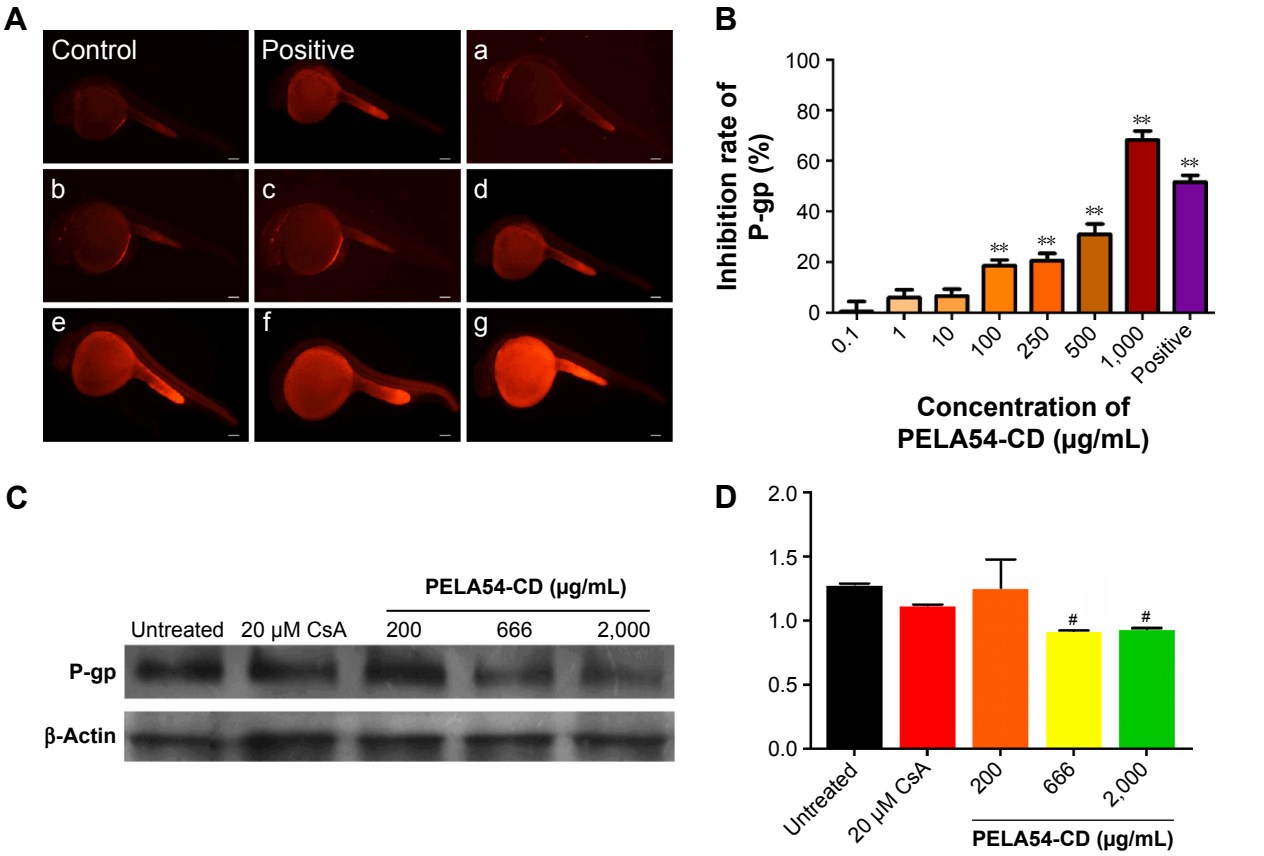

Figure 7 Rhodamine B based P-gp activity assay and P-gp expression in zebrafish.

Notes: (**A**) Rhodamine B accumulation in zebrafish co-treated with a series of concentrations of PELA54-CD. Images under a fluorescence microscope after being co-treated with PELA54-CD and 6 μM Rhodamine B for 20 hours (positive, 1,000 μg/mL CsA). PELA54-CD concentrations (in μg/mL): a, 0.1; b, 1; c, 10; d, 100; e, 250; f, 500; and g, 1,000. Randomly selected ten zebrafish from nine groups were imaged under a stereo fluorescent microscope. Scale bar =100 μm. (**B**) The inhibition rate of P-gp after co-treated with a series of concentrations of PELA54-CD (positive, 1,000 μg/mL CsA). The results are represented as mean ± SE (n=10). Statistical significance (**$P<0.001$) was analyzed comparing with control. (**C**) Twenty-four-hour Western blotting of P-gp. β-Actin was used as internal control, while 20 μM CsA acted as positive control. The concentration of PELA54-CD micelles was 200, 666, and 2,000 μg/mL. (**D**) Densitometry analysis in AB strain wild-type zebrafish. Western blotting was analyzed by ImageJ. The results are represented as mean ± SD (n=3). Statistical significance ($^{\#}P<0.05$) was analyzed comparing with control.

Abbreviations: PELA54, 5:4 monomethoxy poly(ethylene glycol):D,L-lactide; CD, cyclodextrin; CsA, cyclosporine A; P-gp, p-glycoprotein; SE, standard error; SD, standard deviation.

(containing total DOX of 10, 15, or 20 ng) had almost no suppression ability compared with the control group. When the dose increased to 30 ng DOX·HCl, >60% of the zebrafish died. On the contrary, the survival rate in PELA54-CD/DOX-treated groups remained >95%, even when the dose was increased to 30 ng. More interestingly, the fluorescence intensity in groups treated with PELA54-CD/DOX (containing total DOX of 10, 15, 20, or 30 ng) was much weaker than the control group, illustrating that PELA54-CD/DOX could inhibit MCF-7/ADR cell growth in zebrafish model (Figure 8A). The histogram showed that the fluorescence intensity of xenografts decreased with increased DOX dosage after treatment with PELA54-CD/DOX containing 10, 15, or 20 ng DOX compared with the control (Figure 8B). The corresponding inhibition rates of tumor growth reached 28%±1.91%, 47%±2.66%, and 64%±2.66%, for 10, 15, and 20 ng, respectively (Figure 8C). Meanwhile, compared with treatment with free DOX·HCl, the cardiac toxicity of

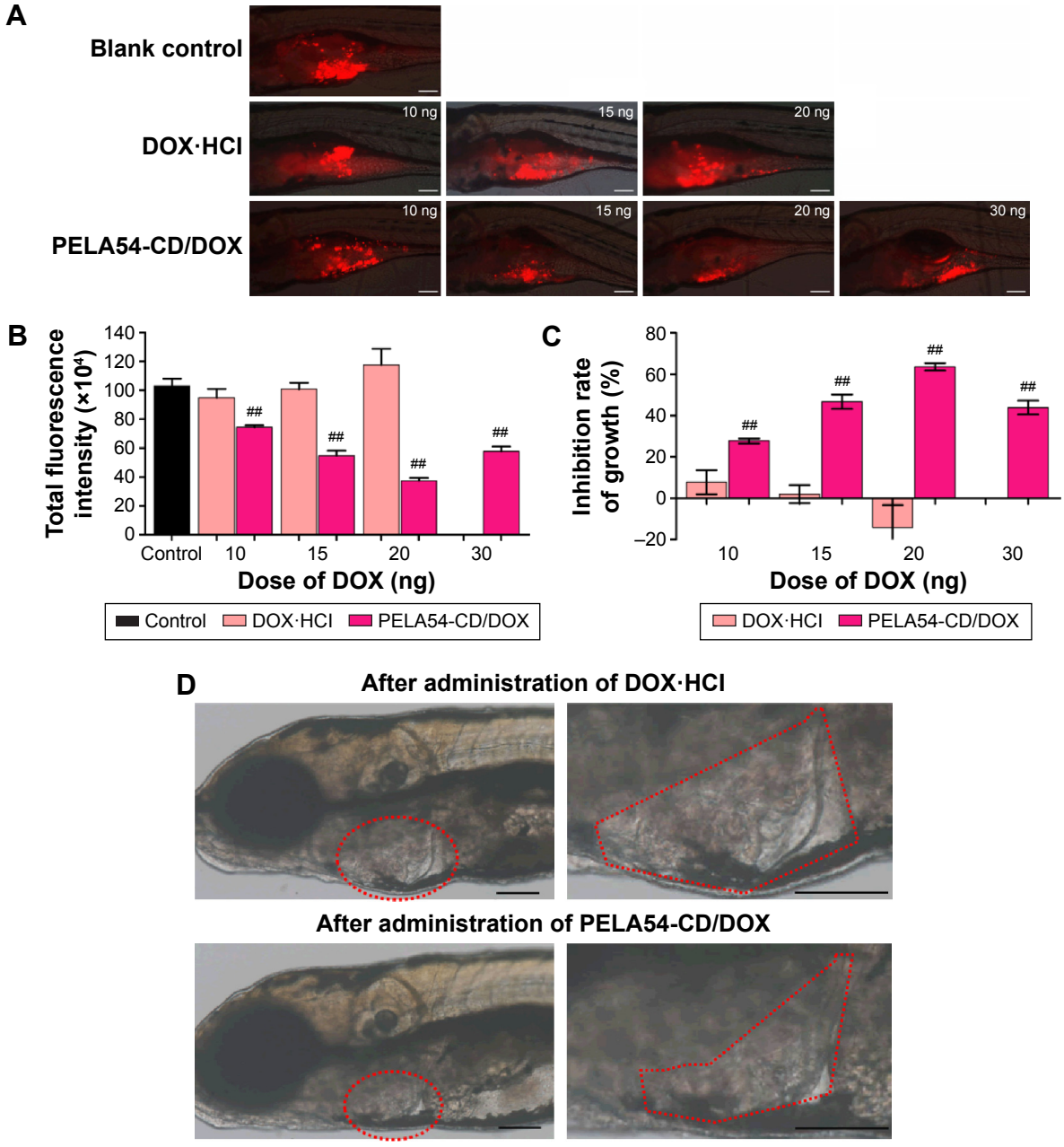

Figure 8 Inhibitory effect on MCF-7/ADR cells and cardiac toxicity of DOX·HCl or PELA54-CD/DOX micelle in zebrafish xenografts.
Notes: (**A**–**C**) Inhibitory effect on MCF-7/ADR cells and (**D**) cardiac toxicity of DOX·HCl or PELA54-CD/DOX micelle in zebrafish xenografts. The results in (**B**) and (**C**) are represented as mean ± SE (n=10). Statistical significance ($^{\#\#}P<0.0001$) was analyzed comparing with control. (**A** and **D**) Scale bar =100 μm. Pericardium of zebrafish shown by red dotted lines.
Abbreviations: DOX, doxorubicin; PELA54, 5:4 monomethoxy poly(ethylene glycol):D,L-lactide; CD, cyclodextrin; SE, standard error.

DOX was much less following PELA54-CD/DOX treatment (Figure 8D). Therefore, PELA54-CD/DOX achieved a expressively higher antitumor efficacy than the same dose of free DOX·HCl and remarkably attenuated cardiotoxicity induced by DOX.

Conclusion

The amphiphilic A-B-C-type polymer of PELA54-CD was synthesized, and DOX-loaded PELA54-CD micelles displayed significantly enhanced tumor suppression effects in vitro and in vivo. It has been confirmed that Pluronic inhibits P-gp and sensitizes MDR cancer cells mainly by means of cellular ATP depletion.[11] However, the action mechanism of PELA54-CD micelle-mediated tumor suppression in both MCF-7/ADR cells and P-gp-overexpressing zebrafish xenograft model was predominantly associated with the increase of P-gp ATPase activity and the inhibition of DOX efflux as a competitive P-gp substrate. Besides, the intracellular ATP depletion and P-gp expression decrease were somewhat involved. β-CD, PEG-CD, PELA54, and PELA54-CD were studied in all of the assays such as cell cytotoxicity, apoptosis, substrate accumulation, ATP depletion, ATPase activity, and protein expression. The results revealed the SAR between the polymeric carriers and drug resistance reversal, and emphasized the importance of integrating three components (β-CD, mPEG5000, PLA) in one polymer molecule to exert synergistic effects on P-gp-mediated DOX sensitization of MCF-7/ADR cancers.

Acknowledgments

This work was supported by the National Natural Science Funds for Excellent Young Scholar (81222047) and National Natural Science Funds (81473173). The authors thank Hangzhou Hunter Biotechnology Inc. for technical assistance with zebrafish models.

Disclosure

The authors report no conflicts of interest in this work.

References

1. Kievit FM, Wang FY, Fang C, et al. Doxorubicin loaded iron oxide nanoparticles overcome multidrug resistance in cancer in vitro. *J Control Release*. 2011;152(1):76–83.
2. Ma B, Chai S, Li N, et al. Reversal of P-glycoprotein-mediated multidrug resistance by a synthetic α-aminoxy peptidomimetic. *Int J Pharm*. 2012;424(1–2):33–39.
3. Xu HB, Li L, Liu GQ. Reversal of multidrug resistance by guggulsterone in drug-resistant MCF-7 cell lines. *Chemotherapy*. 2011;57(1):62–70.
4. Wang F, Zhang D, Zhang Q, et al. Synergistic effect of folate-mediated targeting and verapamil-mediated P-gp inhibition with paclitaxel-polymer micelles to overcome multi-drug resistance. *Biomaterials*. 2011;32(35):9444–9456.
5. Elamanchili P, McEachern C, Burt H. Reversal of multidrug resistance by methoxypolyethylene glycol-block-polycaprolactone diblock copolymers through the inhibition of P-glycoprotein function. *J Pharm Sci*. 2009;98(3):945–958.
6. Liang Z, Wu H, Xia J, et al. Involvement of miR-326 in chemotherapy resistance of breast cancer through modulating expression of multidrug resistance-associated protein 1. *Biochem Pharmacol*. 2010;79(6):817–824.
7. Patil Y, Sadhukha T, Ma L, Panyam J. Nanoparticle-mediated simultaneous and targeted delivery of paclitaxel and tariquidar overcomes tumor drug resistance. *J Control Release*. 2009;136(1):21–29.
8. Gottesman MM, Pastan I. Biochemistry of multidrug resistance mediated by the multidrug transporter. *Annu Rev Biochem*. 1993;62(1):385–427.
9. Georges E, Sharom FJ, Ling V. Multidrug resistance and chemosensitization: therapeutic implications for cancer chemotherapy. *Adv Pharmacol*. 1990;21:185–220.
10. Qiu LY, Yan L, Zhang L, Jin YM, Zhao QH. Folate-modified poly (2-ethyl-2-oxazoline) as hydrophilic corona in polymeric micelles for enhanced intracellular doxorubicin delivery. *Int J Pharm*. 2013;456(2):315–324.
11. Batrakova EV, Li S, Elmquist WF, Miller DW, Alakhov VY, Kabanov AV. Mechanism of sensitization of MDR cancer cells by Pluronic block copolymers: selective energy depletion. *Br J Cancer*. 2001;85(12):1987–1997.
12. Valle JW, Armstrong A, Newman C, et al. A phase 2 study of SP1049C, doxorubicin in P-glycoprotein-targeting pluronics, in patients with advanced adenocarcinoma of the esophagus and gastroesophageal junction. *Invest New Drugs*. 2011;29(5):1029–1037.
13. Wang AZ, Langer R, Farokhzad OC. Nanoparticle delivery of cancer drugs. *Annu Rev Med*. 2011;63(1):185–198.
14. Batrakova EV, Kelly DL, Li S, et al. Alteration of genomic responses to doxorubicin and prevention of MDR in breast cancer cells by a polymer excipient: pluronic P85. *Mol Pharm*. 2006;3(2):113–123.
15. Kabanov AV, Batrakova EV, Alakhov VY. Pluronic block copolymers for overcoming drug resistance in cancer. *Adv Drug Deliv Rev*. 2002;54(5):759–779.
16. Bansal T, Akhtar N, Jaggi M, Khar RK, Talegaonkar S. Novel formulation approaches for optimising delivery of anticancer drugs based on P-glycoprotein modulation. *Drug Discov Today*. 2009;14(21–22):1067–1074.
17. Ji Q, Qiu L. Mechanism study of PEGylated polyester and β-cyclodextrin integrated micelles on drug resistance reversal in MRP1-overexpressed HL60/ADR cells. *Colloids Surf B Biointerfaces*. 2016;144:203–213.
18. Gao M, Xu Y, Qiu L. Enhanced combination therapy effect on paclitaxel-resistant carcinoma by chloroquine co-delivery via liposomes. *Int J Nanomedicine*. 2015;10:6615–6632.
19. Zhang Y, Liu X, Zuo T, Liu Y, Zhang JH. Tetramethylpyrazine reverses multidrug resistance in breast cancer cells through regulating the expression and function of P-glycoprotein. *Med Oncol*. 2012;29(2):534–538.
20. Duan J, Mansour HM, Zhang Y, et al. Reversion of multidrug resistance by co-encapsulation of doxorubicin and curcumin in chitosan/poly (butyl cyanoacrylate) nanoparticles. *Int J Pharm*. 2012;426(1–2):193–201.
21. Schneider E, Horton JK, Yang CH, Nakagawa M, Cowan KH. Multidrug resistance-associated protein gene overexpression and reduced drug sensitivity of topoisomerase II in a human breast carcinoma MCF7 cell line selected for etoposide resistance. *Cancer Res*. 1994;54(1):152–158.
22. Benderra Z, Trussardi A, Morjani H, Villa AM, Doglia SM, Manfait M. Regulation of cellular glutathione modulates nuclear accumulation of daunorubicin in human MCF7 cells overexpressing multidrug resistance associated protein. *Eur J Cancer*. 2000;36(3):428–434.
23. Qiu LY, Wang RJ, Zheng C, Jin Y, Jin le Q. Beta-cyclodextrin-centered star-shaped amphiphilic polymers for doxorubicin delivery. *Nanomedicine(Lond)*. 2010;5(2):193–208.
24. Qiu L, Zhang L, Zheng C, Wang R. Improving physicochemical properties and doxorubicin cytotoxicity of novel polymeric micelles by poly (ε-caprolactone) segments. *J Pharm Sci*. 2011;100(6):2430–2442.

25. Yu JJ, Lee HA, Kim JH, et al. Bio-distribution and anti-tumor efficacy of PEG/PLA nano particles loaded doxorubicin. *J Drug Target*. 2007;15(4):279–284.
26. Dong Y, Feng SS. Methoxy poly(ethylene glycol)-poly(lactide) (MPEG-PLA) nanoparticles for controlled delivery of anticancer drugs. *Biomaterials*. 2004;25(14):2843–2849.
27. Ichi T, Watanabe J, Ooya T, Yui N. Controllable erosion time and profile in poly(ethylene glycol) hydrogels by supramolecular structure of hydrolyzable polyrotaxane. *Biomacromolecules*. 2001;2(1): 204–210.
28. Tang GP, Guo HY, Alexis F, et al. Low molecular weight polyethylenimines linked by beta-cyclodextrin for gene transfer into the nervous system. *J Gene Med*. 2006;8(6):736–744.
29. Zhang L, Lu JF, Jin YM, Qiu LY. Folate-conjugated beta-cyclodextrin-based polymeric micelles withenhanced doxorubicin antitumor efficacy. *Colloid Surface B*. 2014;122:260–269.
30. Xia Q, Wang ZY, Li HQ, et al. Reversion of P-glycoprotein-mediated multidrug resistance in human leukemic cell line by diallyl trisulfide. *Evid Based Complement Alternat Med*. 2012;2012:719805.
31. Liu R, Zhang Y, Chen Y, et al. A novel calmodulin antagonistO-(4-ethoxyl-butyl)-berbamine overcomes multidrug resistance in drug-resistant MCF-7/ADR breast carcinoma cells. *J Pharm Sci*. 2010;99(7): 3266–3275.
32. Shi R, Li W, Zhang X, et al. A novel indirubin derivative PHII-7 potentiates adriamycin cytotoxicity via inhibiting P-glycoprotein expression in human breast cancer MCF-7/ADR cells. *Eur J Pharmacol*. 2011;669(1–3):38–44.
33. Kitchens KM, Kolhatkar RB, Swaan PW, Ghandehari H. Endocytosis inhibitors prevent poly(amidoamine) dendrimer internalization and permeability across Caco-2 cells. *Mol Pharm*. 2008;5(2):364–369.
34. Perry JW, Wobus CE. Endocytosis of murine norovirus 1 into murine macrophages is dependent on dynamin II and cholesterol. *J Virol*. 2010;84(12):6163–6176.
35. Koivusalo M, Welch C, Hayashi H, et al. Amiloride inhibits macropinocytosis by lowering submembranous pH and preventing Rac1 and Cdc42 signaling. *J Cell Biol*. 2010;188(4):547–563.
36. Mo R, Jin X, Li N, et al. The mechanism of enhancement on oral absorption of paclitaxel by N-octyl-O-sulfate chitosan micelles. *Biomaterials*. 2011;32(20):4609–4620.
37. Xu D, Lu Q, Hu X. Down-regulation of P-glycoprotein expression in MDR breast cancer cell MCF-7/ADR by honokiol. *Cancer Lett*. 2006;243(2):274–280.
38. Kimmel CB, Ballard WW, Kimmel SR, Ullmann B, Schilling TF. Stages of embryonic development of the zebrafish. *Dev Dyn*. 1995; 203(3):253–310.
39. Wang Y, Yu L, Han L, Sha X, Fang X. Difunctional Pluronic copolymer micelles for paclitaxel delivery: synergistic effect of folate-mediated targeting and Pluronic-mediated overcoming multidrug resistance in tumor cell lines. *Int J Pharm*. 2007;337(1–2):63–73.
40. Du W, Fan Y, Zheng N, et al. Transferrin receptor specific nanocarriers conjugated with functional 7 peptide for oral drug delivery. *Biomaterials*. 2013;34(3):794–806.
41. Sharma AK, Zhang L, Li S, et al. Prevention of MDR development in leukemia cells by micelle-forming polymeric surfactant. *J Control Release*. 2008;131(3):220–227.
42. Batrakova EV, Li S, Vinogradov SV, Alakhov VY, Miller DW, Kabanov AV. Mechanism of pluronic effect on P-glycoprotein efflux system in blood-brain barrier: contributions of energy depletion and membrane fluidization. *J Pharmacol Exp Ther*. 2001;299(2):483–493.
43. Kabanov AV. Polymer genomics: an insight into pharmacology and toxicology of nanomedicines. *Adv Drug Deliv Rev*. 2006;58(15): 1597–1621.
44. Wesołowska O. Interaction of phenothiazines, stilbenes and flavonoids with multidrug resistance-associated transporters, P-glycoprotein and MRP1. *Acta Biochim Pol*. 2011;58(4):433–448.
45. Brigger I, Dubernet C, Couvreur P. Nanoparticles in cancer therapy and diagnosis. *Adv Drug Deliv Rev*. 2012;64:24–36.
46. Miller DW, Batrakova EV, Waltner TO, Alakhov VYu, Kabanov AV. Interactions of pluronic block copolymers with brain microvessel endothelial cells: evidence of two potential pathways for drug absorption. *Bioconjug Chem*. 1997;8(5):649–657.
47. Conner SD, Schmid SL. Regulated portals of entry into the cell. *Nature*. 2003;422(6927):37–44.
48. Gamboa JM, Leong KW. In vitro and in vivo models for the study of oral delivery of nanoparticles. *Adv Drug Deliv Rev*. 2013;65(6):800–810.
49. Perumal OP, Inapagolla R, Kannan S, Kannan RM. The effect of surface functionality on cellular trafficking of dendrimers. *Biomaterials*. 2008;29(24–25):3469–3476.
50. Yin L, Tang H, Kim KH, et al. Light-responsive helical polypeptides capable of reducing toxicity and unpacking DNA: toward nonviral gene delivery. *Angew Chem Int Ed Engl*. 2013;52(35):9182–9186.
51. Chiu YL, Ho YC, Chen YM, et al. The characteristics, cellular uptake and intracellular trafficking of nanoparticles made of hydrophobically-modified chitosan. *J Control Release*. 2010;146(1):152–159.
52. Doige CA, Sharom FJ. Transport properties of P-glycoprotein in plasma membrane vesicles from multidrug-resistant Chinese hamster ovary cells. *Biochim Biophys Acta*. 1992;1109(2):161–171.
53. Katzir H, Yeheskely-Hayon D, Regev R, Eytan GD. Role of the plasma membrane leaflets in drug uptake and multidrug resistance. *FEBS J*. 2010;277(5):1234–1244.
54. Alakhova DY, Rapoport NY, Batrakova EV, et al. Differential metabolic responses to pluronic in MDR and non-MDR cells: a novel pathway for chemosensitization of drug resistant cancers. *J Control Release*. 2010;142(1):89–100.
55. Aller SG, Yu J, Ward A, et al. Structure of P-glycoprotein reveals a molecular basis for poly-specific drug binding. *Science*. 2009;323(5922): 1718–1722.
56. Borgnia MJ, Eytan GD, Assaraf YG. Competition of hydrophobic peptides, cytotoxic drugs, and chemosensitizers on a common P-glycoprotein pharmacophore as revealed by its ATPase activity. *J Biol Chem*. 1996;271(6):3163–3171.
57. Garrigues A, Nugier J, Orlowski S, Ezan E. A high-throughput screening microplate test for the interaction of drugs with P-glycoprotein. *Anal Biochem*. 2002;305(1):106–114.
58. Litman T, Skovsgaard T, Stein WD. Pumping of drugs by P-glycoprotein: a two-step process? *J Pharmacol Exp Ther*. 2003;307(3):846–853.
59. Ambudkar SV, Dey S, Hrycyna CA, Ramachandra M, Pastan I, Gottesman MM. Biochemical, cellular, and pharmacological aspects of the multidrug transporter. *Annu Rev Pharmacol Toxicol*. 1999;39(1): 361–398.
60. Fong WF, Shen XL, Globisch C, et al. Methoxylation of 3′,4′-aromatic side chains improves P-glycoprotein inhibitory and multidrug resistance reversal activities of 7,8-pyranocoumarin against cancer cells. *Bioorg Med Chem*. 2008;16(7):3694–3703.
61. Lineweaver H, Burk D. The determination of enzyme dissociation constants. *J Am Chem Soc*. 1934;56(3):658–666.
62. Nicholson C. Interaction between diffusion and Michaelis-Menten uptake of dopamine after iontophoresis in striatum. *Biophys J*. 1995; 68(5):1699–1715.
63. Healey FP. Slope of the Monod equation as an indicator of advantage in nutrient competition. *Microb Ecol*. 1980;5(4):281–286.
64. Wang RB, Kuo CL, Lien LL, Lien EJ. Structure-activity relationship: analyses of p-glycoprotein substrates and inhibitors. *J Clin Pharm Ther*. 2003;28(3):203–228.
65. Zamora JM, Pearce HL, Beck WT. Physical-chemical properties shared by compounds that modulate multidrug resistance in human leukemic cells. *Mol Pharmacol*. 1988;33(4):454–462.
66. Sachs-Barrable K, Thamboo A, Lee SD, Wasan KM. Lipid excipients Peceol and Gelucire 44/14 decrease P-glycoprotein mediated efflux of rhodamine 123 partially due to modifying P-glycoprotein protein expression within Caco-2 cells. *J Pharm Pharm Sci*. 2007;10(3):319–331.
67. Loo TW, Bartlett MC, Clarke DM. Simultaneous binding of two different drugs in the binding pocket of the human multidrug resistance P-glycoprotein. *J Biol Chem*. 2003;278(41):39706–39710.

68. Young S, Parker PJ, Ullrich A, Stabel S. Down-regulation of protein kinase C is due to an increased rate of degradation. *Biochem J*. 1987;244(3):775–779.
69. Mimeault M, Batra SK. Emergence of zebrafish models in oncology for validating novel anticancer drug targets and nanomaterials. *Drug Discov Today*. 2013;18(3–4):128–140.
70. Nicoli S, Ribatti D, Cotelli F, Presta M. Mammalian tumor xenografts induce neovascularization in zebrafish embryos. *Cancer Res*. 2007; 67(7):2927–2931.